UNIVERSITÀ DEGLI STUDI DI PADOVA

Dipartimento di Fisica e Astronomia “Galileo Galilei”

Corso di Laurea in Fisica

Tesi di Laurea

Study of discrete symmetry in ^{21}Ne

Relatore

Dr. Daniele Mengoni

Correlatore

Prof. Lorenzo Fortunato

Laureando

Edoardo Buonocore

Anno Accademico 2019/2020

Abstract

Since their first conceptualization in the work of J.A. Wheeler, nucleons clusters have been invistigated thoroughly. In recent years, R. Bijker, F. Iachello and V. Della Rocca used the Cluster Shell-Model framework to describe light nuclei seen as k α-particles disposed on a specific lattice plus n nucleons. The objective of this thesis is to extend for the first time their approach to the case of ^{21}Ne. The geometrical model describing the nucleus and its intrinsic symmetry are presented, followed by a brief excursus on numerical calculations. In addition, single-particle states in the resulting cluster field are investigated. Moreover, a methodology towards the optimization of the parameters describing the model, the results obtained, and the corresponding level scheme are presented and described. In conclusion the cluster shell-model level scheme and the experimental one are compared.

Ringrazio il mio relatore Dr. Daniele Mengoni e il Prof. Lorenzo Fortunato per tutto il sostegno e il tempo dedicatomi in questo progetto.

Contents

1 Introduction

Since the beginning of Nuclear Physics history, nucleons clusters have been used as effective tools in the description of different phenomena. In 1937, after the observation of the large binding energy characteristic of α-particles, J. A. Wheeler[1] formalized a method (Resonating Group Structure Method **RGSM**) to describe light nuclei in terms of small clusters of nucleons. With a novel approach to Nuclear Physics, he grouped together protons and neutrons into strongly bound sub-structures, with the aim of describing the nucleus total wave-function as an antisymmetrized combination of the wave functions of the different sub-structures.
Wheeler's seminal paper was soon followed by the work of R. L. Hafstad and E. Teller[2] who, adapting Wheeler's description in terms of α-clusters, showed that the binding energy depends linearly on the number of bonds between the clusters in the structures describing light nuclei up to ^{32}**S**. They also noticed that Wheeler's **RGSM** becomes more and more inefficient as the Mass number of the nucleus increases. Throughout the years, the cluster nature of light nuclei has been the topic of many studies. A brief summary of the works in the study of nucleons clusters includes, but it is not limited to:

1. K. Ikeda et al. in *The systematic structure changes into the molecule-like structures in the 4n self-conjugate nuclei*(an example of Ikeda Diagram in Fig. 1)[3];
2. D.M. Brink with the *Generator Coordinate Method* **GCM**[4];
3. S. Saito with the *Orthogonality Condition Model* **OCM**[5];
4. R. Bijker and F. Iachello in *Cluster states in nuclei as representations of a U(ν+1) group*[6];

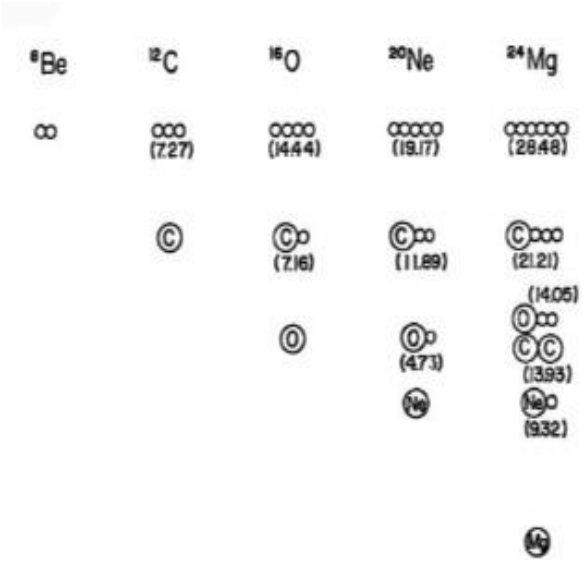

Figure 1: *Ikeda Diagram. Excitation Energy expressed in MeV[3].*

In 1970, Brink and collaborators[7] suggested configurations for the ground states of nuclei composed of k α-particles (up to k=7 with ^{28}**Si**, Fig. 2). For k=2,3,4, for example, they proposed respectively the following: a dumbell with Z_2 symmetry ($^{8}_{4}$**Be**), an equilateral triangle with D_{3h} symmetry ($^{12}_{6}$**C**) and a tetrahedron with T_d symmetry ($^{16}_{8}$**O**). In recent years, R. Bijker, F. Iachello and V. Della Rocca[8, 9, 10] have been carrying out extensive theoretical investigations on isotopes of k α-particles nuclei for k=2,3,4 plus 1 nucleons ($^{9}_{4}$**Be**, $^{9}_{5}$**B**, $^{13}_{6}$**C**, $^{17}_{8}$**O**). This original thesis is to be intended as an extension of the recent work of V. Della Rocca, R. Bijker and F. Iachello to the case of the ^{21}**Ne** in the cluster shell model. From an experimental point of view, both the rotational spectrum and the electromagnetic transition rates show that ^{21}**Ne** displays collective behavior.
The fact that the experimental bands with $K^P = \frac{1}{2}^+$ and $K^P = \frac{1}{2}^-$ are parity doubled ($\Delta E \approx 5\ KeV$ as can be seen in Fig. 2) suggests that the collective behaviour comes from a cluster behavior rather than a quadrupole or octupole deformation.

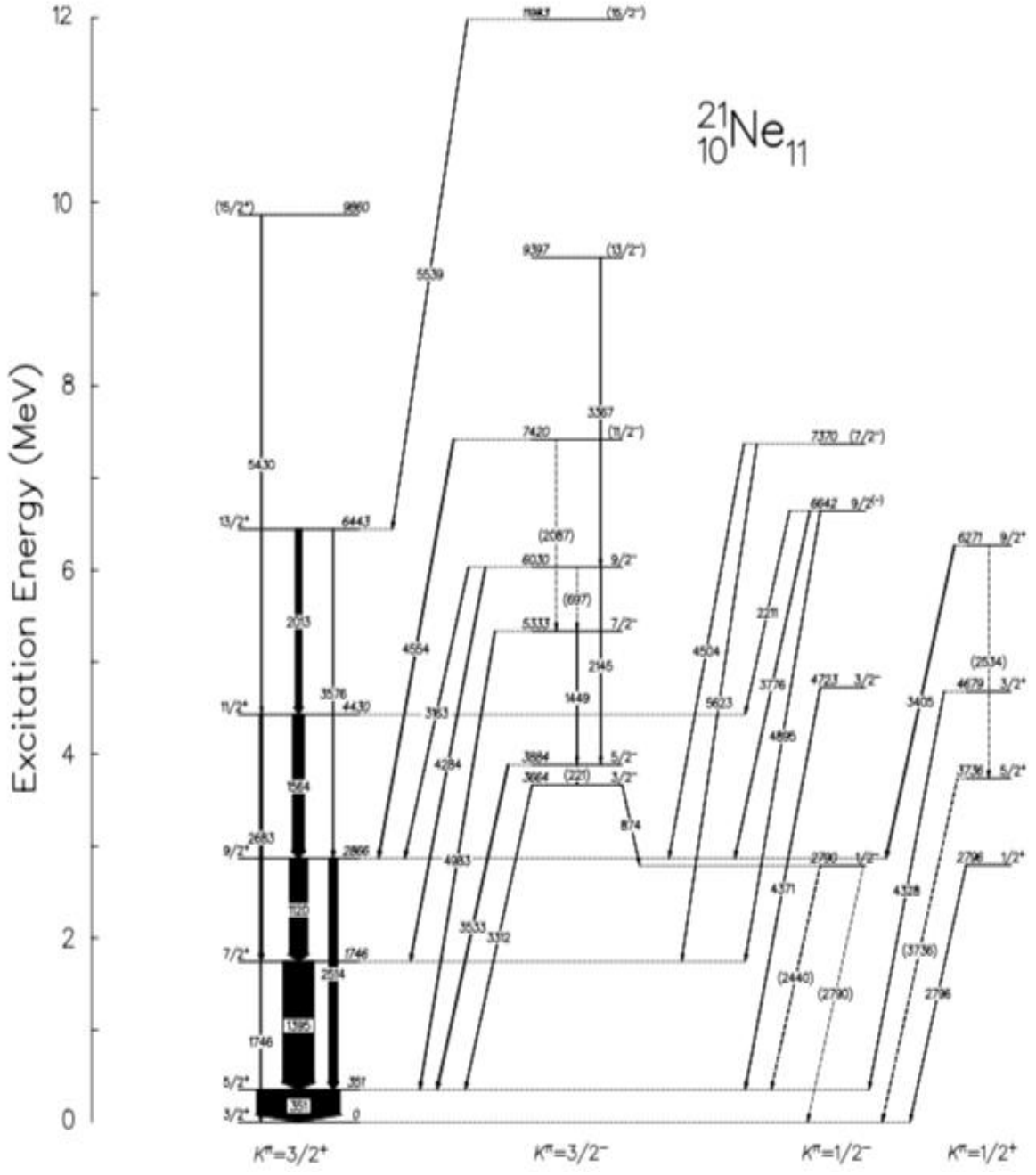

Figure 2: *Partial level scheme for the cluster bands* ^{21}**Ne**. *The widths of the arrows are proportional to intensity. Dashed arrow indicates transitions tentatively observed[11].*

2 Geometrical model and algebraic symmetry

The theoretical framework under which this thesis takes shape is called Cluster Shell model. In this framework, the majority of the binding energy is stored in the different sub-groups, whilst the remaining energy allows the single sub-structures to be weakly bound together in the cluster structure.

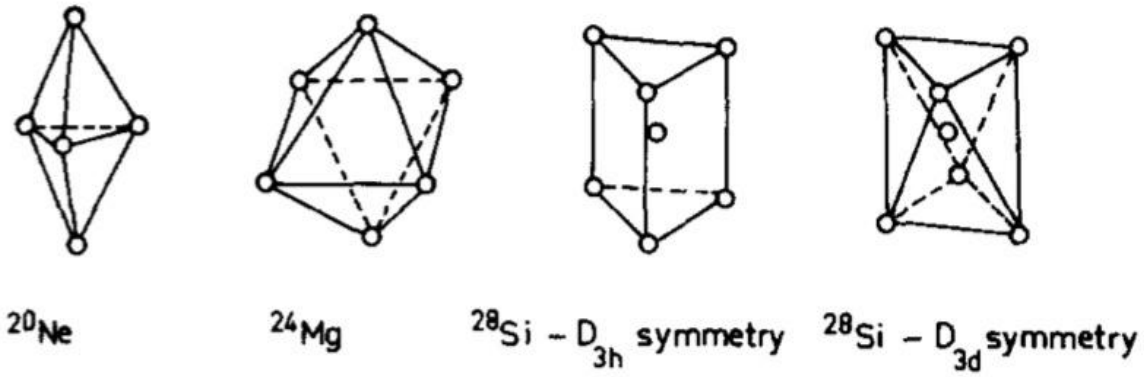

Figure 3: *Alpha-particle configuration for some 4n nuclei[7].*

Following the ideas in reference [7] (Fig. 3), $^{20}_{10}$**Ne** is assumed to be composed of 5 α-particles located at the vertices of a triangular bi-pyramid in analogy with the structure known in the VESPR theory (Valence Shell Electron Pair Repulsion) for molecules such as $\mathbf{PCl_5}$. Under the assumption that the addition of a neutron doesn't change the α-lattice, the symmetry of the cluster potential of ^{21}**Ne** is considered unaltered from the one of ^{20}**Ne**.

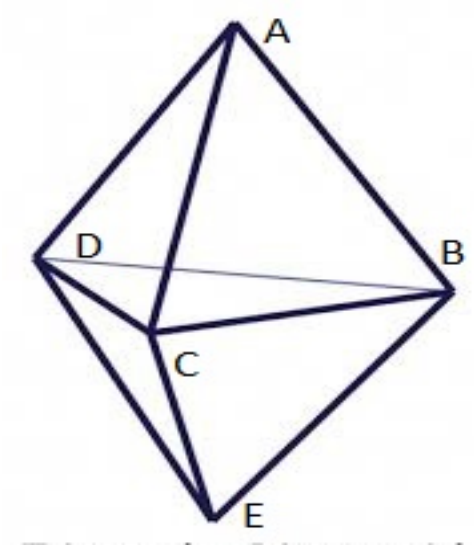

Figure 4: *triangular bi-pyramid.*

The triangle **BCD** is equilateral (Fig. 4) with **O** its barycenter. The geometrical model is described by three parameters:

1. β describes the length of the segment **OB** (being the triangle **BCD** equilateral, the three segments **OB**,**OC** and **OD** are congruent, so the choice in the definition of β is arbitrary);
2. h adimensional parameters defined as the ratio between the length of the segment **OA** and β;
3. δ describes the asymmetry of the structure by defining the length of the segment **OE** as $\beta(h + \delta)$

For the purposes of this thesis the parameters h and δ are set to the values such that all α-particles are equidistant from the point **O**, which is the center of mass CM of the system for this choice of h and δ.

$$h = 1 \qquad \delta = 0 \tag{2.1}$$

The core structure described above has D_{3h} symmetry and so does the resulting cluster potential.

2.1 Cluster density

It is assumed that the density of each α-particle is described by the following Gaussian function of the coordinates:

$$\rho_\alpha = (\frac{a}{\pi})^{\frac{3}{2}} e^{-ar^2} \tag{2.2}$$

where $a = 0,56 fm^{-2}$ (obtained by fitting the form factor data from electron scattering [12]) for a free α-particle.
Considering a frame of reference with its origin in the geometrical barycenter of the triangle **BCD**, let $\vec{\mathbf{r}}_i$ be the position vector identifying the i-th α in the lattice . The density of the core structure is, therefore, given by the following:

$$\rho(\vec{\mathbf{r}}) = (\frac{a}{\pi})^{\frac{3}{2}} \sum_{i=1}^{5} e^{-a(\vec{\mathbf{r}}^2 - \vec{\mathbf{r}}_i^{\,2})} \tag{2.3}$$

The Eq. (2.3) can be used both as charge and mass density after having it normalized to the total charge and mass of the core structure (Z=10, A=20). By setting, in spherical coordinates:
$\vec{\mathbf{r}_1} = (h\beta, 0, 0)$; $\vec{\mathbf{r}_2} = (\beta, \frac{\pi}{2}, 0)$; $\vec{\mathbf{r}_3} = (\beta, \frac{\pi}{2}, \frac{\pi}{3})$; $\vec{\mathbf{r}_4} = (\beta, \frac{\pi}{2}, \frac{2\pi}{3})$; $\vec{\mathbf{r}_5} = ((h+\delta)\beta, \pi, 0)$.
For the choice of the parameters h and δ, the radial components of $\vec{\mathbf{r}}_i$ is β for i=1,...,5.

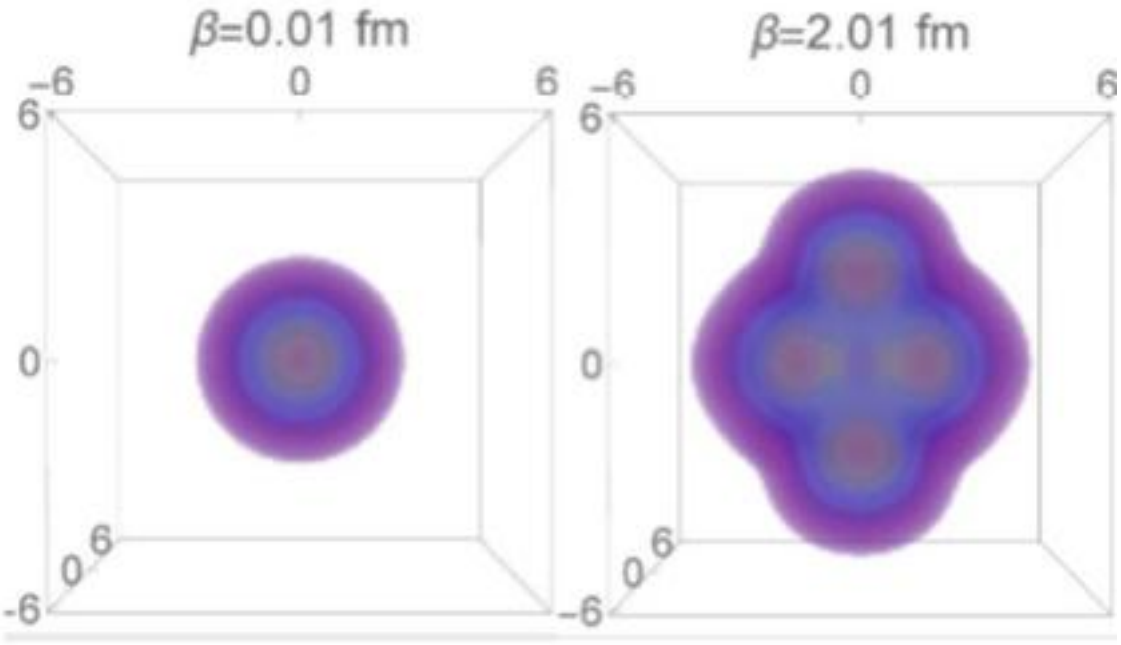

Figure 5: *Density of the 5 α-cluster structure at two different values of the parameter* β.

The choice made in the definitions of the different $\vec{\mathbf{r}}_i$ allows the model to reproduce with continuity a spherical density centered in the CM for $\beta = 0$ and the situation in which the clusters are completely apart for $\beta \to \infty$. The density plot in Fig. 5 shows both the spherical density for $\beta = 0$ and the trigonal bypiramid structure for $\beta > 0$, i.e. $\beta = 2.01 fm$.

2.2 Potential and Hamiltonian

The potential generated by the 5-cluster structure is given by the convolution of the multipole expansion of the density (Eq. 2.4) with the interaction among nucleons $v(\vec{\mathbf{r}} - \vec{\mathbf{r}}')$ chosen as a

Volkov-type Gaussian potential in the calculations[13].[1]

$$\rho(\vec{\mathbf{r}}) = (\frac{a}{\pi})^{\frac{3}{2}} e^{-a(r^2+\beta^2)} 4\pi \sum_{l,m} i_l(2ar\beta) Y_l^m(\theta,\phi) \sum_{i=1}^{5} (Y_l^m(\theta,\phi))^* \tag{2.4}$$

$$V(\vec{\mathbf{r}}) = -V_0 e^{-a_V(r^2+\beta^2)} 4\pi \sum_{l,m} i_l(2a_V r\beta) Y_l^m(\theta,\phi) \sum_{i=1}^{5} (Y_l^m(\theta,\phi))^* \tag{2.5}$$

Even though the two expressions might seem identical, but for a multiplicative factor, actually only their dependence on the spherical coordinates is identical. As a matter of fact, the two parameters a and a_V are different, respectively related to the density Gaussian and the the Volkov-type interaction Gaussian[13]. Next, we consider the motion of a neutron in the cluster field generated by the 5α-particles core structure $V(\vec{\mathbf{r}})$ in Eq. (2.5). The Hamiltonian of the neutron is:

$$H = H_0 + V(\vec{\mathbf{r}}) + V_{ls} \tag{2.6}$$

where $H_0 = \frac{p^2}{2m}$ is the free-particle field and $V_{ls} = V_{0,ls}\vec{\mathbf{s}} \cdot (-\vec{\nabla} V \times \vec{\mathbf{p}})$ is the spin-orbit interaction. For the choice of the parameters δ and h, the α-clusters are on a sphere. Therefore, the angular derivative contributions are negligible, allowing the following expression for the spin-orbit interaction: $V_{ls} = V_{0,ls}\frac{1}{r}\frac{\partial V}{\partial r}(\vec{\mathbf{s}} \cdot \vec{\mathbf{l}})$. The symmetry of the Hamiltonian is defined by the symmetry group of $V(\vec{\mathbf{r}})$, which is itself defined by the configuration of the clusters. Therefore, the Hamiltonian has D_{3h} point symmetry. Let Φ be the wavefunction of the neutron, HΦ=EΦ. It can be expanded in terms of the harmonic oscillator eigenfunctions basis

$$\Phi = \sum_{nljm} c_{nljm} \phi_{nljm}(\vec{\mathbf{r}}) \tag{2.7}$$

The oscillator length ν has to be set so as to define properly the basis. In order to set ν a Gaussian, a Wood-Saxon and a harmonic oscillator potentials were matched in r=0 and $r = R_{0,WS} = 1.2A^{\frac{1}{3}}$[10], obtaining:

$$\nu = \sqrt{\frac{mc^2 V_0}{4\hbar^2 c^2}} A^{-\frac{1}{3}} fm^{-2} \tag{2.8}$$

In summary, the model is described by the following free-parameters: $\beta, h, \delta, V_0, and V_{0,ls}$ (h and δ were fixed to reduce the complexity of the calculations in this first attempt).

2.3 Numerical calculations excursus

The eigenvalues problem for H has been solved numerically. In order to solve it, the harmonic oscillator basis had to be truncated by fixing the value of n_{max} and l_{max}.A preliminary test of convergence was conducted by increasing the value of n_{max} and l_{max} progressively. Even though the higher these values are set, the higher the precision of the result, in order to have reasonable computation time, n_{max} and l_{max} were set respectively to 8 and 5. This choice ensured a sufficiently good convergence for the intervals spanned varying the free-parameters. Increasing n_{max} would indeed improve the results on the order of few hundreds of KeV while drastically increasing the computation time. Since positive eigenvalues are relative to unbound states which would require a scattering theory outside of the model, to the scope of this thesis only negative eigenvalues and the relative eigenfunction expansions in the truncated basis are considered.

[1] $i_l(x) = \frac{J_l(ix)}{i^l}$ is the modified spherical Bessel function

3 Single-particle states in cluster potential

In opposition to the limiting case $\beta \to 0$ where the clusters merged together resulting in a Gaussian well potential with spherical symmetry (group $\mathbf{O(3)}$), it is expected that, for non-null values of β (β>0), the single-particle energy levels are splitted accordingly to the symmetry introduced in the system by the cluster potential (group $\mathbf{D_{3h}}$). In this chapter, after a brief discussion about the point group symmetry and its representations, through correlation diagrams, the trend of single-particle energy levels of a fermion in cluster potential with $\mathbf{D_{3h}}$ symmetry as a function of β is shown and discussed.

3.1 Elements of Group Theory

The definition of *representation* of a group is introduced:

Definition 1. *Representation of a group*
Let G be a group, a representation of G is a homomorphic mapping between all elements g of G and a set of Operators D(g) acting on a vector space V, compatible with G inner products: $D(g_1 \circ g_2) = D(g_1)D(g_2)$.

The action of the operators D(g) onto a vector $\vec{\mathbf{v}} \in V$ describes how $\vec{\mathbf{v}}$ transforms under the action of the element $g \in G$. Representations are not unique and the same group could be described with a variety of different representations. For the purposes of this thesis only matrix representations are considered.

Definition 2. *Reducible, fully reducible, and irreducible representations*
Let G be a group. Fixed $g \in G$, its representation D(g) is said:

1. *reducible* if it can be written as a block superior triangular matrix;
2. *fully reducible* if it can be written as a block diagonal matrix;
3. *irreducible* otherwise;

When a representation is fully reducible, it is used the following notation[10]:

$$D(g) = \sum_i D_i(g) \tag{3.1}$$

Expression (3.1) is not supposed to be read as a proper sum, but as a block diagonal matrix, where D_i are the building blocks. Since the matrix form of D(g) depends on the choice of basis, a representation is identified by its *characters*, a set of number invariant under change of basis.

3.2 Group O(3) and splitting of its representations

A group extremely important in physics is **O(3)**, which describes the rotation of a system in 3 dimensions. Let $R(\alpha, \beta, \gamma)$ be a matrix representation of a rotation in **O(3)**.[10] The transformation of the spherical harmonics $Y^l_m(\theta, \phi)$ under $R(\alpha, 0, 0)$ is known:

$$R(\alpha, 0, 0)Y^l_m(\theta, \phi) = e^{-im\alpha}Y^l_m(\theta, \phi) \tag{3.2}$$

It can be found that for a generic rotation:

$$R(\alpha, \beta, \gamma)Y^l_m(\theta, \phi) = \sum_{m'=-l}^{l} Y^l_{m'}(\theta, \phi)D^l_{m'm}(\alpha, \beta, \gamma) \tag{3.3}$$

where $D^l_{m'm}(\alpha,\beta,\gamma)$ denotes the $m'm$ element of the matrix representation of the rotation. The characters of $R(\alpha,0,0)$ are also well known:

$$\chi^l(\alpha) = \frac{\sin\left((l+\frac{1}{2})\alpha\right)}{\sin\frac{\alpha}{2}} \tag{3.4}$$

where $l \in \mathbb{N}$. Moreover, the character of the class of the identity (α=0), which is $\chi^l(0) = 2l+1$, coincides with the dimension of the representation $D^l(R)$. When considering particles with spin $s = \frac{1}{2}$, it is necessary to consider **SO(3)** covering group, **SU(2)**, whose characters are:

$$\chi^j(\alpha) = \frac{\sin\left((j+\frac{1}{2})\alpha\right)}{\sin\frac{\alpha}{2}} \tag{3.5}$$

with $j \in \{\frac{n}{2}, n \in \mathbb{N}\}$ When j assumes non-negative half integer values, one element of **SO(3)** is the image through an homomorphism f:**SU(2)**→**SO(3)** of two different elements of **SU(2)**, which are related to the double-valued representations of **SO(3)**. In order to predict the splitting of the spherical energy levels due to the cluster potential symmetry of a fermion, it is of interest to find the representation of the *double (extended) group of* $\mathbf{D_{3h}}$ contained in **SU(2)**. Indeed, it can be shown that a fully reducible representation D(G) of a group G can be decomposed in terms of irreducible represenatations D(G′) of a group G′ contained in G

$$D(G) = \sum_\nu a^\nu D_\nu(G') \tag{3.6}$$

where a^ν is the number of times each representation of G′ are repeated in the decomposition[14]. It can be proven that a^ν are all integers and are related to the characters of the representation by the following:

$$a^\nu = \frac{1}{g}\sum_i g_i \chi_i \chi_i^{*(\nu)} \tag{3.7}$$

where χ_i and $\chi_i^{*(\nu)}$ are respectively the characters of the two groups considered, g is the order of G′ and g_i is the number of elements in the class i. Even though these relations do not hold in the case of double-valued representations, it is possible to extend them using the homomorphism between **SO(3)** and **SU(2)**. Specifically, for integer j, the characters of the D^j representation coincide with those of D^l, therefore the representations are equivalent. For j half-integer,to each matrix D^l are associated both D^j and $-D^j$, which correspond to the double values representation of **O(3)**. In this way, being D^j single valued in **SU(2)**, it is possible to use Eqs. (3.6) and (3.7).

3.3 D_{3h} group and double valued representation

The dihedral group with an horizontal plane of reflection $\mathbf{D_{3h}}$ has 12 elements in 6 classes.

1. E, identity class, 1 element
2. σ_h, pure reflections in an horizontal plane, 1 element
3. σ_v, pure reflections in a vertical plane, 3 elements
4. C_2, class of rotation of an angle of π,3 elements
5. S_6 and S_6^2, classes of the rotation-reflection symmetry, 4 elements[2]

[2]The class S_6^2 coincides with C_3

Its extended group $\mathbf{D'_{3h}}$ consists of adding to the elements of $\mathbf{D_{3h}}$ all of its elements composed with a rotation R of 2π, where $R \neq E$ in **SU(2)** topology. $\mathbf{D'_{3h}}$ has 24 elements in 9 classes. Therefore there are 3 (number of classes of $\mathbf{D'_{3h}}$ minus number of classes of $\mathbf{D_{3h}}$) double valued representations. These representations satisfy[3]:

$$12 = \sum_{i=1}^{3} n_i^2 \tag{3.8}$$

where $n_i \in \mathbb{N}$ is the dimension of the i-th double-valued representation. This is satisfied only if $n_i = 2, \ \forall i = 1,2,3$. Therefore there are three bidimensional double valued irreducible representations E'_i (Using Mulliken symbols conventions). The character table of the group $\mathbf{D'_{3h}}$ is presented in table I.

$\mathbf{D'_{3h}}$	E	R	C_6 C_6^5R	C_6^2 C_6^4R	C_6^5 C_6R	C_6^4 C_6^2R	C_6^3 C_6^3R	C_2 C_2R	$C_{2'}^3$ $C_{2'}R$
E'_1	2	-2	$\sqrt{3}$	1	$-\sqrt{3}$	-1	0	0	0
E'_2	2	-2	$-\sqrt{3}$	1	$\sqrt{3}$	-1	0	0	0
E'_3	2	-2	0	-2	0	2	0	0	0

Table 1: *Character table of the group* $\mathbf{D'_{3h}}$. *Classes with the same characters are displayed on two different lines.*

From the character table and the application of Eqs. (3.6), and (3.7) follows immediately the splitting of the representation D^j of **O(3)**:

$$D^{\frac{1}{2}} = E'_1 \tag{3.9}$$

$$D^{\frac{3}{2}} = E'_1 + E'_3 \tag{3.10}$$

$$D^{\frac{5}{2}} = E'_1 + E'_2 + E'_3 \tag{3.11}$$

$$D^{\frac{7}{2}} = E'_1 + 2E'_2 + E'_3 \tag{3.12}$$

$$D^{\frac{9}{2}} = E'_1 + 2E'_2 + 2E'_3 \tag{3.13}$$

$$D^{\frac{11}{2}} = 2E'_1 + 2E'_2 + 2E'_3 \tag{3.14}$$

and so on for higher values of j.

3.4 Correlation diagrams

Plotting the different single-particle energy levels as a function of β, the following trends are expected to be found:

1. in the limiting case $\beta \to 0$ the clusters are merged together and the resulting potential has spherical symmetry and the energy levels can be labelled using the spherical shell model quantum numbers

2. for β>0 the levels are splitted accordingly to the double valued representation of the point group D_{3h} in **O(3)**. The physical meaning of Eqs. (3.9) to (3.15) is immediate. If a rotationally invariant system is inserted into a field with D_{3h} symmetry it is expected that a $j = \frac{1}{2}$ state doesn't split, a $j = \frac{3}{2}$ state split into two states, a $j = \frac{5}{2}$ state split into three, and so on. Moreover, for β>0 each energy level is twice degenerate with $\pm$K (projection of the total angular momentum J) as expected from a time reversal invariant Hamiltonian.

[3] 12 because there are 12 additional elements in the passage to the double group

3. In the opposing limiting case $\beta \to \infty$ the clusters are completely separated and the energy levels can be interpreted as those of 5 separated Gaussian wells each labelled by the usual spherical shell model notation and energy value decreased of a factor $\frac{1}{5}$ with respect to the β=0 case.

A correlation diagram for a deep and wide potential ($V_0 = 30MeV, V_{0,ls} = 12MeVfm^2, \alpha = 0,051fm^-2$) is reported in Fig. 6

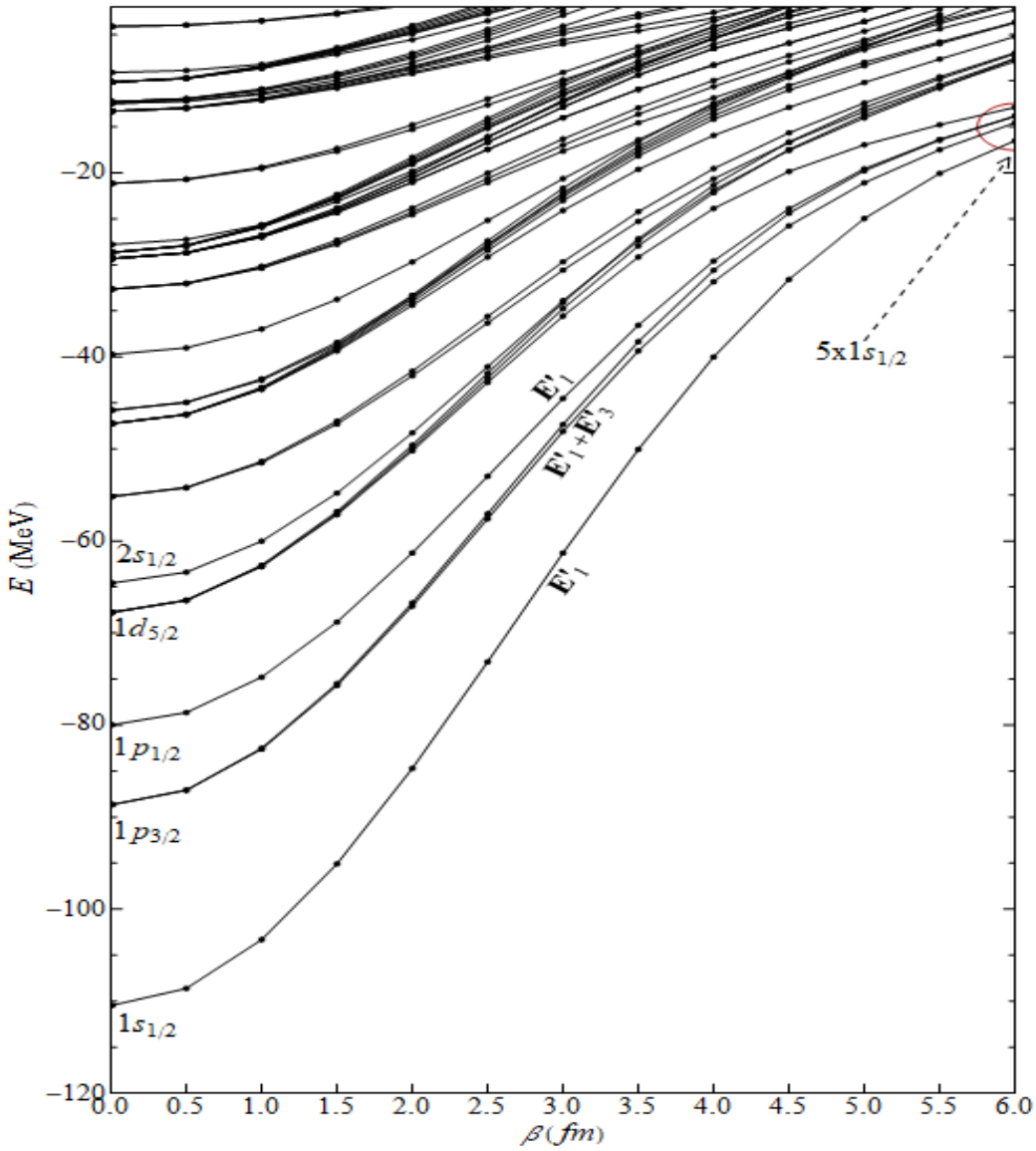

Figure 6: *Energy levels of a spin $\frac{1}{2}$ particle in a D_{3h} symmetric potential generated by 5 α-particles with $V_0 = 30MeV, V_{0,ls} = 12MeVfm^2, \alpha = 0,051fm^-2$.*

4 Methodology and result

In this chapter the concepts presented previously are applied to the case of **^{21}Ne**. Moreover, to the scope of this thesis only the rotational bands were calculated and a preliminary level scheme is presented, while no calculations were made regarding electromagnetic transitions and form factors.

4.1 Methodology

In order to decide whether or not the proposed model agrees in a satisfactory manner with the experimental level scheme, it is necessary to choose a set of values for the free-parameters. In particular, for each set of values of $V_0, V_{0,ls}$ the intrinsic energies of the rotational bands were evaluated in the following fashion:

1. Eigenvalues and the eigenvector expansion in the truncated basis are evaluated for values of β from 0 to 6 fm with finite steps of 0,25 fm.

2. The Correlation Diagram for $V_0, V_{0,ls}$ is drawn and each state is labelled by $|\Omega, K, P\rangle$. Ω labels the representations of D_{3h}, K is the projection of the total angular momentum J on a body fixed axis and P the parity. In particular, for each one of the spinor representation[9] the allowed values of K^P are given by:

$$\Omega = E_1' \qquad K^P = \frac{1}{2}^+ \quad and \quad K^P = (3n \pm \frac{1}{2})^{(-)^n} \tag{4.1}$$

$$\Omega = E_2' \qquad K^P = \frac{1}{2}^- \quad and \quad K^P = (3n \pm \frac{1}{2})^{(-)^{n+1}} \tag{4.2}$$

$$\Omega = E_3' \qquad K^P = (3n \pm \frac{3}{2})^{\pm} \tag{4.3}$$

   with $n = 0, 1, 2, ...$, J=K, K+1,K+2,... and K>0. To be noted the double degeneracy for $K^P = K^{\pm}$ for the representation E_3' (parity doubling).

3. Following the usual rules for the placing of fermions in different states, the ground state is determined. The parameter β is fixed at the value which gives the minimum difference between the resulting ground state energy and the separation energy of a neutron in **^{21}Ne** ($S_n = 6761.16 KeV$) and the intrinsic energies of the rotational bands are assigned as the single particle energy levels at the fixed value of β.

Each set of values for the parameters is associated with a set of three values $\Delta E_{\frac{3}{2}^- \to \frac{3}{2}^+}$, $\Delta E_{\frac{1}{2}^- \to \frac{3}{2}^+}$, $\Delta E_{\frac{1}{2}^+ \to \frac{3}{2}^+}$. which can be compared with the experimental values (Fig. 2) through the following quantity:

$$\sigma^2 = (\Delta E^{exp}_{\frac{3}{2}^- \to \frac{3}{2}^+} - E^{th}_{\frac{3}{2}^- \to \frac{3}{2}^+})^2 + (\Delta E^{exp}_{\frac{1}{2}^- \to \frac{3}{2}^+} - E^{th}_{\frac{1}{2}^- \to \frac{3}{2}^+})^2 + (\Delta E^{exp}_{\frac{1}{2}^+ \to \frac{3}{2}^+} - E^{th}_{\frac{1}{2}^+ \to \frac{3}{2}^+})^2 \tag{4.4}$$

Firstly, this process was iterated for V_0 from 5 MeV to 35 MeV with steps of 5 MeV and $V_{0,ls}$ fixed at 12 MeV fm^2. Secondly, to allow a more precise prediction the same process was evaluated for V_0 from 8 MeV to 12 MeV with steps of 1 MeV and $V_{0,ls}$ from 8 MeV fm^2 to 24 MeV fm^2 with steps of 2 MeV fm^2. In conclusion, the free parameters are set to the values which minimize σ:

$$V_0 = 10 \ MeV \qquad V_{0,ls} = 14 \ MeV fm^2 \qquad \beta = 1,75 \ fm \tag{4.5}$$

4.2 Rotational Bands

Due to the collective motion of the system, on each single-particle level found are built rotational bands. Because of the symmetry of the model, the projection K of the angular momentum along the symmetry axis is a good quantum number and the energy levels, under the rigid rotor assumption, are given by:

$$E_{rot}(\Omega, K, J) = \epsilon_\Omega + \frac{\hbar^2}{2I_x}[J(J+1) + b_\Omega K^2] \tag{4.6}$$

where ϵ_Ω is the intrinsic energy, $I^{^{21}\mathrm{Ne}}$ is the moment of inertia, b_Ω is a rotational constant.

4.2.1 Intrinsic Energy

The intrinsic energies of the rotational bands are given by the single-particle energy levels numerically calculated for the parameters that minimize σ(Table 2).

$K^P = \frac{3}{2}^-$	$K^P = \frac{5}{2}^+$	$K^P = \frac{1}{2}^+$	$K^P = \frac{1}{2}^-$
5,874	0,108	0,894	5,789

Table 2: *Intrinsic energy of the excited rotational bands for* ^{21}***Ne****. All values are in MeV.*

4.2.2 Moment of Inertia

The (classical) analytical expressions for I_i^{core} is evaluated considering Gaussian, rather than point-like, α-particle:

$$I_x^{core} = \frac{Am}{a} + \frac{7Am\beta^2}{10} \tag{4.7}$$

$$I_y^{core} = \frac{Am}{a} + \frac{7Am\beta^2}{10} \tag{4.8}$$

$$I_z^{core} = \frac{Am}{a} + \frac{3Am\beta^2}{5} \tag{4.9}$$

Where A=20 is the mass number for the core(Table 3), and $a = 0.56fm^{-2}$.

$\frac{I_x^{core}}{m}$	$\frac{I_y^{core}}{m}$	$\frac{I_z^{core}}{m}$
78,6	78,6	72,5

Table 3: *Cluster Core contribution to the total moment of Inertia. All Values in* fm^2.

The moment of inertia $I^{^{21}\mathrm{Ne}}$ of ^{21}Ne is obtained[10] by adding the momentum of inertia of the odd neutron I_i^n to that of the core

$$I_i^{^{21}\mathrm{Ne}} = I_i^{core} + I_i^n \tag{4.10}$$

where I_i^n is obtained by evaluating its expectation value on each level χ_Ω:

$$I_x^n = m\int (y^2 + z^2)|\chi_\Omega|^2 d^3\vec{\mathbf{r}} \tag{4.11}$$

$$I_y^n = m\int (x^2 + z^2)|\chi_\Omega|^2 d^3\vec{\mathbf{r}} \tag{4.12}$$

$$I_z^n = m\int (y^2 + x^2)|\chi_\Omega|^2 d^3\vec{\mathbf{r}} \tag{4.13}$$

In table 4 the evaluation of the momentum of Inertia I_i^n and I_i for the final choice of parameters.

	$K^P = \frac{3}{2}^+$	$K^P = \frac{3}{2}^-$	$K^P = \frac{1}{2}^+$	$K^P = \frac{1}{2}^-$	$K^P = \frac{5}{2}^+$
$\frac{I_x^n}{m}$	13,5	20,9	14,8	25,7	11,3
$\frac{I_y^n}{m}$	13,5	20,9	14,8	25,7	11,3
$\frac{I_z^n}{m}$	12,4	27,8	16,1	18,7	16,9
$\frac{I_x^{^{21}\mathrm{Ne}}}{m}$	92,1	99,5	93,4	104,3	89,8
$\frac{I_y^{^{21}\mathrm{Ne}}}{m}$	92,1	99,5	93,4	104,3	89,9
$\frac{I_z^{^{21}\mathrm{Ne}}}{m}$	84,9	100,3	88,6	91,2	89,4

Table 4: *Odd neutron contribution to the moment of Inertia and* ^{21}**Ne** *moment of Inertia. All values are in* fm^2.

4.2.3 Rotational Constant

The rigid rotor Hamiltonian is:

$$\hat{H_R} = \sum_i^3 \frac{\hat{J_i^2}}{2I_i^{^{21}\mathrm{Ne}}} \tag{4.14}$$

$$I_x^{^{21}\mathrm{Ne}} = I_y^{^{21}\mathrm{Ne}} \neq I_z^{^{21}\mathrm{Ne}} \neq 0 \tag{4.15}$$

Therefore the Hamiltonian can be written as:

$$\hat{H_R} = \frac{1}{2I_x^{^{21}\mathrm{Ne}}} \left[\hat{\vec{\mathbf{J}}}^2 + \left(\frac{I_x^{^{21}\mathrm{Ne}}}{I_z^{^{21}\mathrm{Ne}}} - 1 \right) \hat{J_z}^2 \right] \tag{4.16}$$

In Eq. (4.16) appears the expression for the rotational constant. As a matter of fact, applying to a state $|J, K\rangle$ the Hamiltonian operator one obtains the expression for the energy levels in the rotational bands in Eq. (4.6), but for an additive factor (Intrinsic Energy).

$$b_\Omega = \frac{I_x^{^{21}\mathrm{Ne}}}{I_z^{^{21}\mathrm{Ne}}} - 1 \tag{4.17}$$

In table 5 the rotational constants are shown for the different rotational bands.

	$K^P = \frac{3}{2}^+$	$K^P = \frac{3}{2}^-$	$K^P = \frac{1}{2}^+$	$K^P = \frac{1}{2}^-$	$K^P = \frac{5}{2}^+$
b_Ω	0,0715	0,0653	0,0699	0,0621	0,0738

Table 5: *Coriolis parameters of the rotational bands for* ^{21}**Ne**. *All values are adimensional.*

4.3 Results

A comparison is drawn between experimental energy levels and theoretical ones calculated through Eqs. (4.6), in Figure 7 and 8.

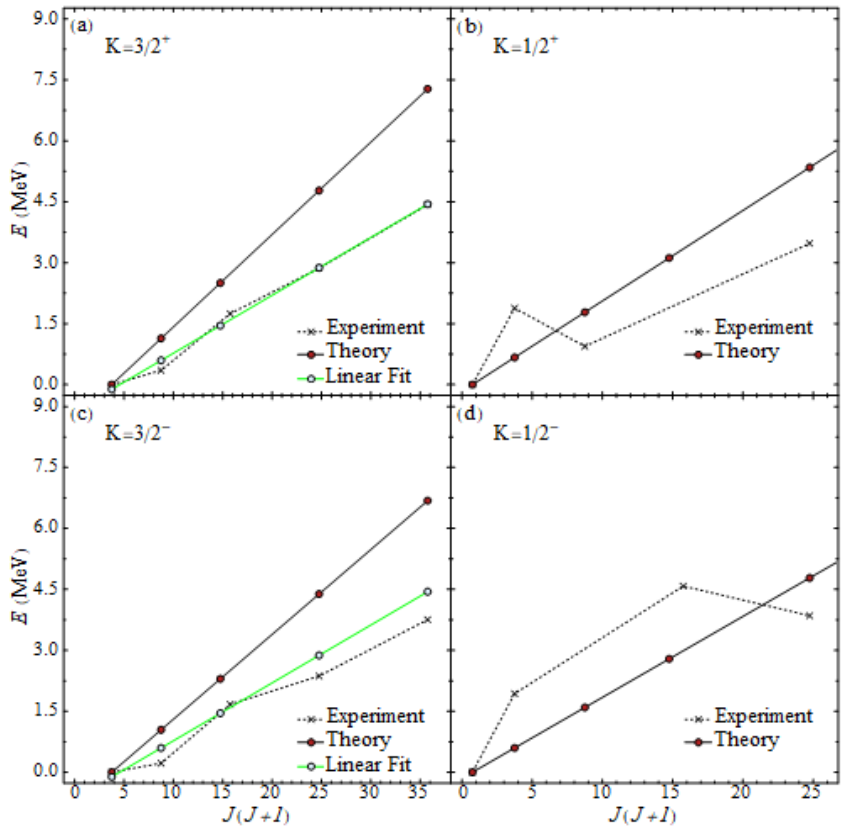

Figure 7: *Energy levels are plotted as a function of J(J+1) for bands with* $K^P = \frac{3}{2}^{\pm}, \frac{1}{2}^{\pm}$. *A comparison is drawn between experimental values and theoretical calculations.*

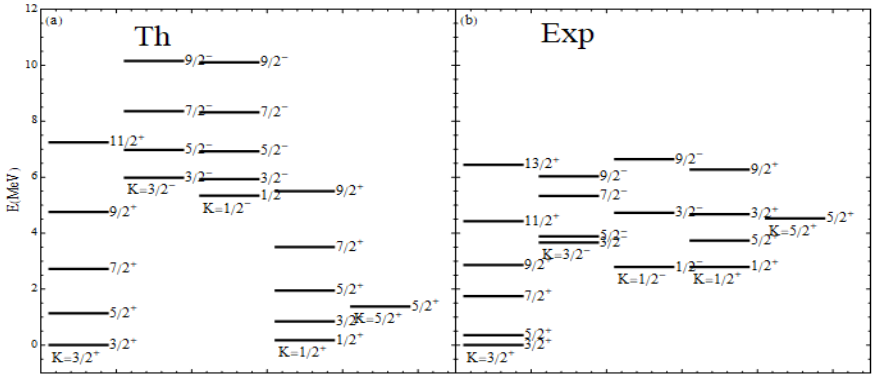

Figure 8: *Experimental and theoretical energy level schemes for* ^{21}Ne.

The Diagrams show the following features:

1. **Figure 7 panels (a) and (c)**: The rigid rotor appears to be a good assumption for the $K^P = \frac{3}{2}^+$ and $K^P = \frac{3}{2}^-$ bands, but for the presence of staggering. The theoretical prediction for the moment of inertia $I_x^{^{21}\mathrm{Ne}}$ is less than the value obtained by the fitting of the experimental value for both bands.[Evidence *a*]

2. **Figure 7 panels (b) and (d)**: the discordance between experimental and theoretical rotational bands is evident. The experimental values clearly do not depend linearly on J(J+1).[Evidence *b*]

3. **Figure 8**: there are different aspects under which the theoretical and experimental level schemes do not agree. In the theoretical level scheme the $K^P = \frac{1}{2}^+$ headband appears almost degenerate with the Ground state. [Evidence *c*] In the Experimental $K^P = \frac{1}{2}^+$ band the level relative to $J = \frac{5}{2}$ is lower in energy than the $J = \frac{3}{2}$, which is a feature not found in the theoretical prediction. [Evidence *d*] Moreover the energy predicted for the $K^P = \frac{3}{2}^-$ and $K^P = \frac{1}{2}^-$ headbands are larger than the experimental data. [Evidence *e*]

Evidence *b* and *d* could be explained by the addition of a decoupling term[10] to Eq. (4.6):

$$E_{rot}(\Omega, K, J) = \epsilon_\Omega + \frac{\hbar^2}{2I_x^{^{21}\mathrm{Ne}}}[J(J+1) + b_\Omega K^2 + \delta_{K,\frac{1}{2}} a_\Omega (-1)^{j+\frac{1}{2}}(j+\frac{1}{2})] \tag{4.18}$$

where the so-called decoupling parameter a_Ω is defined as:

$$a_\Omega = -\sum_{nlj}(-1)^{j+\frac{1}{2}}(j+\frac{1}{2})\left|c^\Omega_{nlj\frac{1}{2}}\right|^2 \tag{4.19}$$

where $c^\Omega_{nlj\frac{1}{2}}$ are the coefficients of the wavefunction expansion.

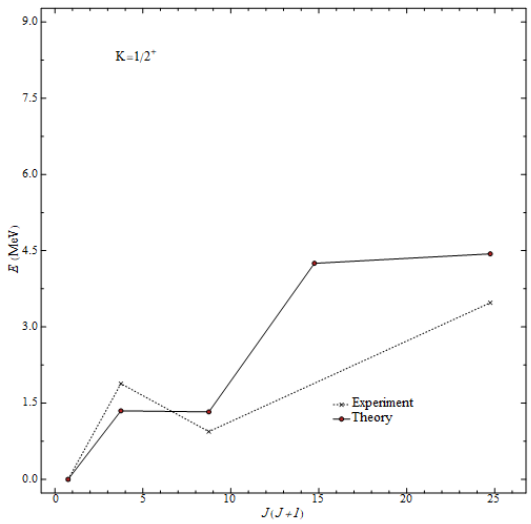

Figure 9: *Energy levels are plotted as a function of J(J+1) for bands with* $K^P = \frac{1}{2}^+$. *A comparison is drawn between experimental values and theoretical predictions with the decoupling term.*

A tentative calculation of a_Ω only for the $K^P = \frac{1}{2}^+$ bands is made. The resulting energy levels are plotted in Fig. 9. Evidence *c* and *e* could be explained by a change of paradigm in

the attribution of K^P to the different representations. Instead of looking at the single-particle wavefunction expansions and assign to each level the appropriate K^P, Eq. (4.1), (4.2) and (4.3) could be interpreted as different bands built on the same representation for different values of n, i.e. the E'_3 of the ground state can be interpreted as the $K^P = \frac{3}{2}^+$ band over which is built $K^P = \frac{3}{2}^-$(n=1). The analytical expression for the core contribution to the momentum of Inertia in the general case is:

$$I_x^{core} = \frac{Am}{a} + \frac{Am\beta^2}{10}(5 + 2h^2 + 4h\delta + 2\delta^2) \tag{4.20}$$

$$I_y^{core} = \frac{Am}{a} + \frac{Am\beta^2}{10}(5 + 2h^2 + 4h\delta + 2\delta^2) \tag{4.21}$$

$$I_z^{core} = \frac{Am}{a} + \frac{3Am\beta^2}{5} \tag{4.22}$$

Evidence *a* points toward a larger momentum of Inertia which could be achieved by studying the model at different values of h>1 or δ>0.

5 Conclusions

The model presented is self-consistent. The chosen symmetry is able to predict the ground state $\frac{3}{2}^+$ of **^{21}Ne**, but the level scheme predicted by the model does not agree with the experimental data. The trigonal bipyramid structure proposed by Brink et al. [7] with h=1 and δ=0 appears to be inconclusive. Even though this choice of parameters should be investigated with the alternative paradigm for the assignment of the intrinsic energies (Section 4.3) to properly refuse the hypotheses, the necessity for a larger moment of inertia would still be unaccounted for without changing also the value of the geometrical parameters h and δ. Therefore, it is suggested to continue this investigation firstly for h>1, and eventually for δ>0, where the rotational bands are described by Eq. (4.18) and the intrinsic energies deriving from the application of the alternative paradigm. Another possibility could be to investigate other geometric structure, resulting in a different point group symmetry, i.e. a twisted bow-tie like structure corresponding to a D_{2d} group antiprismatic symmetry.

References

[1] J. A. Wheeler. "On the mathematical description of light nuclei by the method of resonating group structure". In: *Physical Review, 52* (Dec. 1937), pp. 1107–1122.

[2] L. R. Hafstad and E. Teller. "The alpha particle model of the nucleus". In: *Physical Review, 54* 63 (Nov. 1938), pp. 681–692.

[3] K. Ikeda, N. Takigawa, and H. Horiuchi. "The systematic structure change into the molecule-like structures in the self-conjugate *4n* nuclei". In: *Supplement of the Progress of Theoretical Physics, Extra Number* (1968), pp. 464–475.

[4] D. M. Brink. "The alpha particle model of light nuclei". In: *Procedings of the international School E. Fermi-Varenna* (1966), pp. 247–277.

[5] S. Saito. "Interaction between clusters and pauli principle". In: *Progress of Theoretical Physics,41* (1969), pp. 705–722.

[6] R. Bijker and F. Iachello. "Cluster states in nuclei as representations of a U(ν+1) group". In: *Physical Review C, 61:067305* 92 (May 2000).

[7] D. M. Brink et al. "Investigation of the alpha particle model for light nuclei". In: *Physics Letter B, 33* (1970), p. 143.

[8] V. Della Rocca, R. Bijker, and F. Iachello. "Single-particle levels in cluster potentials". In: *Nuclear Physics A, 966* (June 2017), pp. 158–184.

[9] R. Bijker and F. Iachello. "Evidence for triangular $\mathbf{D'_{3h}}$ Symmetry in ^{13}C". In: *Physical Review Letters, 122* (Apr. 2019).

[10] V. Della Rocca. "Cluster Structure of light nuclei". In: *Gran Sasso Science Institute, Ph.D. Thesis* (2017).

[11] C. Wheldon et al. "Octuple-deformed molecular bands in ^{21}Ne". In: *European Physical Journal A 26* (2005), pp. 321–326.

[12] I. Sick, J.S. McCarthy, and R.R. Whitney. In: *Phys. Lett. B, 64* (1976), p. 33.

[13] A. B. Volkov. In: *Nucl. Phys.74* (1965), p. 33.

[14] M. Hamermesh. *Group theory and its application to physical problems*. Addison-Wesley Publishing company, 1962.